IJE TRANSACTIONS B: Applications Vol. 33, No. 11, (November 2020) 2146-2154

International Journal of Engineering

Journal Homepage: www.ije.ir

Behavior of Eccentrically Inclined Loaded Ring Footings Resting on Granular Soil

A. H. Sadeghi Fazel, J. Bolouri Bazaz*

Department of Civil Engineering, Faculty of Engineering, Ferdowsi University of Mashhad, Mashhad, Iran

P A P E R I N F O

Paper history:
Received 10 May 2020
Received in revised form 12 August 2020
Accepted 07 September 2020

Keywords:
Combined Loading
Experimental Modeling
Failure Envelope
Ring Footing
Sand

A B S T R A C T

For civil engineers, the determination of ring footing bearing capacity subject to the combination of inclined and eccentric loading is a great topic of interest. In this paper, a novel approach is proposed to predict the behavior of ring footing subject to combinations of inclined and eccentric loading using the failure envelope approach, which can explain shallow footings behavior. Load eccentricity, inclination angle, and diameter ratio for ring footings are the most effective parameters on the failure envelope. In this regard, a series of experiments were conducted to investigate the behavior of ring footing subject to a possible form of eccentrically inclined loading. Three values of diameter ratio were considered, including n = 0.2, 0.4, and 0.6, along with a circular footing (n = 0). According to the test results, the conical 3D failure envelope and its equation were developed for each type of footing model. With constant vertical load the failure envelopes show that when the eccentricity is increased, the possible inclination angle is decreased. Also, by increasing the vertical loading, the possible eccentricity and inclination angle is decreased. Based on the observations, and obtained failure envelopes for different diameter ratios, when a ring footing is subject to combined eccentric inclined loading, n=0.4 is optimum. In the following, by using the failure envelope, the concepts of critical eccentricity and critical inclination angle were defined in a way that is suitable for studying the stability of ring footings in the V-H-M/B space.

***doi**: 10.5829/ije.2020.33.11b.04*

NOMENCLATURE

n	Ring footing diameter ratio	D_o	Outer diameter of ring footing
e	Vertical eccentericity	D_i	Inner diameter of ring footing
e_h	Horizontal eccentericity	V_{ult}	Ultimate vertical load
V	Vertical load	α	Inclination angel of inclined load
H	Horizontal load	R_f	Reduction factor of eccentric loading
M	Bending moment	H_{ult}	Ultimate horizontal load
B	Diameter of footing model	M_{ult}	Ultimate bending moment

1. INTRODUCTION

Foundations of structures may be subjected to inclined and eccentric loading depending on various design considerations. Ring footing is a special type of shallow foundation that is appropriate for telecommunication towers, silos, bridge piers, and advertisement boards. Classical researchers provided empirical coefficients when an eccentric or inclined load is applied on a footing [1–3]. Several studies about ring footing using different methods have been performed. Using experimental model, the ring footing behavior, subject to vertical loading was investigated. The results showed that the behavior of ring footing would approach a strip footing for n>0.7 [4]. The optimum value of ring footing bearing capacity occurred when the diameter ratio was 0.4 [5, 6]. The results of the behavior of small-scale ring footings subject to eccentric loading on reinforced soil reported

*Corresponding Author Institutional Email: *bolouri@um.ac.ir* (J. Bolouri Bazaz)

Please cite this article as: A. H. Sadeghi Fazel, J. Bolouri Bazaz, Behavior of Eccentrically Inclined Loaded Ring Footings Resting on Granular Soil, International Journal of Engineering (IJE), IJE TRANSACTIONS B: Applications Vol. 33, No. 11, (November 2020) 2146-2154

that with an increase in eccentricity, the bearing capacity ratio of ring footing increased more than circular foundation. Also, for an optimum response of ring footing, the recommended diameter ratio is 0.39 [7]. Based on the limit equilibrium method, the solution was derived for the bearing capacity of a ring footing on soil beds [8]. Besides that, the bearing capacity factor, Nγ, was calculated by using the stress characteristic method [9]. After conducting in-situ tests, the bearing capacity of circular and ring plate was investigated in very dense calcareous sands using plate load tests. The results showed that the bearing capacity of ring footings is greater than that of circular footings with the same outer diameter in some situations [10]. In other work, researchers found that by increasing the diameter ratio, the bearing capacity of ring footings resting on clay was reduced [11]. In numerical simulations, the bearing capacity of a ring footing was assessed using a finite difference method on non-cohesive soil subject to eccentric load [12].

In the field of non-vertical-central loading on a shallow footing, the stability analysis of an eccentrically loaded footing supported by sand was proposed by using the slices method [13]. The theoretical limit equilibrium analysis was performed to determine the average ultimate bearing capacity of strip footing subject to eccentrically-inclined load [14]. About 120 laboratory test results have been reported regarding the ultimate bearing capacity of a strip footing subject to eccentrically-inclined load as a reduction factor [15]. There are many papers about the application of analytical and numerical approaches in the modeling of shallow footings subject to general loading [16–24].

Since the ring footing of many structures such as telecommunication towers and silos is subject to combination of eccentric inclined load, it is necessary experimentally to investigate the behavior of this type of footing. Besides that, most of the literature reviewed in the previous section focused on the effect of diameter ratio on the settlement and bearing capacity of ring footings subject to vertical load. Also, both experimental and theoretical research has been conducted on ring footings to find an optimum diameter ratio. However, to the best of the authors' knowledge, no attempt has been made to produce a model explaining the behavior of ring footings subject to a combination of inclined, eccentric, and vertical loading, which is useful for designing the structure subject to aforementioned loading. To this aim, six loading states were defined to investigate the behavior of ring footings resting on sand in V/V_{ult}-tan(α)-e/B space. In this space, the instability conditions of footings, in addition to bearing capacities, subjected to inclined and eccentric loading under constant and variable inclination angles and eccentricity were studied.

2. PROGRAM DEFINITION

The combination of vertical, inclined, and eccentric loading was considered to investigate the effect of loading states on ring footing bearing capacity. The six loading states are defined as follows:

V state: The pure central vertical loading (Figure 1a) is applied to determine the ultimate bearing capacity, V_{ult}, of the ring footing.

α_V state: The central vertical load is applied up to $0.2V_{ult}$, $0.3V_{ult}$, $0.5V_{ult}$, $0.7V_{ult}$, and $0.85V_{ult}$. While keeping the vertical load constant, the horizontal load is applied and gradually increased until reaching failure (H/V=variable) (Figure 1b).

α_C state: Vertical and horizontal loads are applied to the center of the footing model with a constant ratio (H/V=constant). The result of this loading state is inclined load with a constant inclination angle of α (Figure 1c).

e_V state: The eccentric loading with variable eccentricity is applied to the footing model. Similar to the V-H path, the central vertical load was increased until reaching $0.3V_{ult}$, $0.5V_{ult,}$ and $0.7V_{ult}$, while keeping the vertical load constant, the moment was applied on the footing as a couple (Figure 1d).

e_C state: The vertical loading with a constant eccentricity (e) is applied to the footing model (Figure 1-e).

α_V-e_V state: The inclined eccentric loading with a variable inclination angle and eccentricity is applied to the footing model. The central vertical load was increased until reaching $0.3V_{ult}$, $0.5V_{ult}$, and $0.7V_{ult}$, while keeping the vertical load constant, the bending moment by the horizontal load with a constant ratio was gradually applied to the ring footing until reaching failure (Figure 1f).

A load-displacement curve was drawn for all of the experiments, and the failure point was derived for each test. Since the sandy soil used in this study had a medium density, no peak was observed in the load-displacement

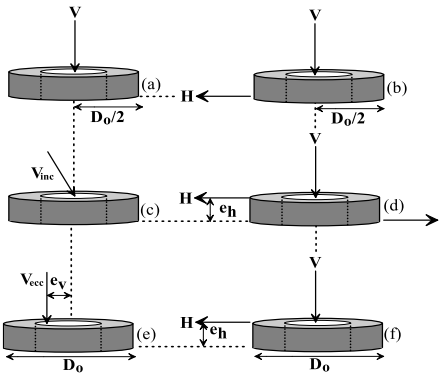

Figure 1. The position of loads in different loading states

curves. The failure criterion for whole loading states was considered when the slope load-displacement curve was approaching zero (i.e., the curve tends to become a straight line). For example, the load-displacement results of the $\mathbf{e_c}$ loading state for the ring footing n=0.4 is illustrated in Figure 2.

If all of the failure-relevant points are perceived, a failure envelope in V/V_{ult}-tan(α)-e/B space is established, which is useful for design engineers. For instance, by considering constant and variable inclination angles and eccentricity, the influence of eccentricity and inclination can be observed simultaneously. A unique failure envelope obviously exists for each diameter ratio of ring footings with specific soil parameters. The purpose of this research is to obtain the equation of the failure envelope in V/V_{ult}-tan(α)-e/B space and the parameters involved in it. The flowchart of this research methodology is illustrated in Figure 3. Based on the above explanation, the test details are summarized in Table 1.

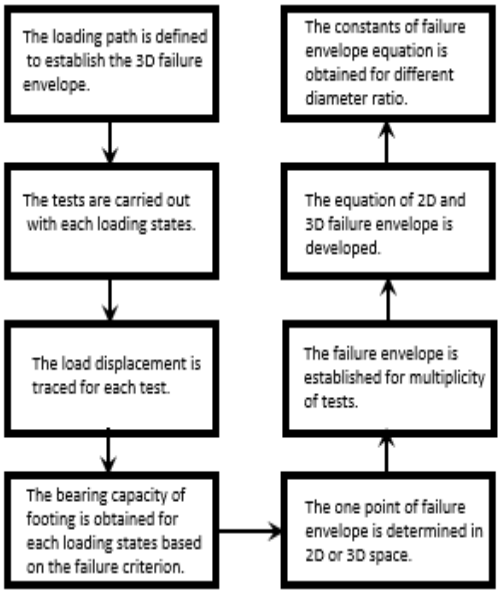

Figure 3. The flowchart of research methodology

3. LOADING SYSTEM

The loading system is suitable to apply precisely the combination of vertical load, horizontal load, and bending moment simultaneously. Since the vertical and horizontal loads are incrementally applied by filling the cylindrical tanks with constant water flow, the magnitude of the applied load was measured precisely by the water entered at the rate of 10 liters per minute. Additionally, two calibrated load cells were employed to measure and ensure no error was induced during load application. The schematic drawing of the apparatus is shown in Figure 4; the picture of loading system is illustrated in Figure 5. When the desired loading combination is achieved. It is of interest to apply horizontal load or a bending moment with either a constant or variable angle or eccentricity, respectively; which is achieved by the automated drain valves. Fully lubricated frictionless rolling bearings facilitate the movement of the reservoir tanks easily to create vertical and horizontal eccentricities [25].

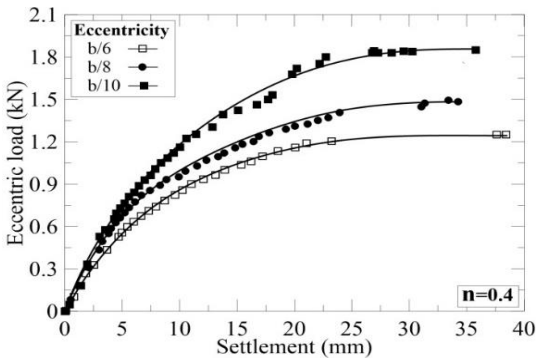

Figure 2. The typical load-displacement results of the $\mathbf{e_c}$ loading state for ring footing (n=0.4)

3. 1. Sample Preparation The experimental model tests were conducted in a steel tank made with 1000 mm high, 1100 mm inside dimension and 10 mm thickness. The loading system was firmly attached to the top of the tank. The tank diameter was larger than 5 times the footing diameter (20 cm) to avoid undesirable effect of the test tank boundary on the results [12].

3. 2. Soil Specifications The soil used in this research was dry Firuzkuh sand (No. 161), which was taken from north of Iran. It is a uniform sand with a specific gravity of G_s=2.71 and maximum and minimum

TABLE 1. Main characteristics of tests program

Series	No. of tests	Loading State	V/V_{ult}	e	α(Degree)	e_h(mm)	n
1	4	V	-	-	-	-	0, 0.2, 0.4, 0.6
2	20	α_V	0.2, 0.3, 0.5 ,0.7, 0.85	-	variable	-	0, 0.4, 0.4, 0.6
3	8	α_C	-	-	18,24	-	0, 0.2, 0.4, 0.6
4	20	e_V	0.2, 0.3, 0.5, 0.7, 0.85	variable	-	50	0, 0.2, 0.4, 0.6
5	12	e_C	-	B/10,B/8,B/6	-	-	0, 0.2, 0.4, 0.6
6	36	α_V-e_V	0.7, 0.5, 0.3	-	-	50,100,200	0, 0.2, 0.4, 0.6

dry unit weights of γ_{max}=16.4 kN/m^3 and γ_{min}=14.1 kN/m^3, respectively. A pluviation system that has been developed at Mashhad University was employed to prepare a sand bed with a medium relative density of 70%. The corresponding dry unit weight and internal friction angle were γ=15.2 kN/m^3 φ=36^o, respectively [26].

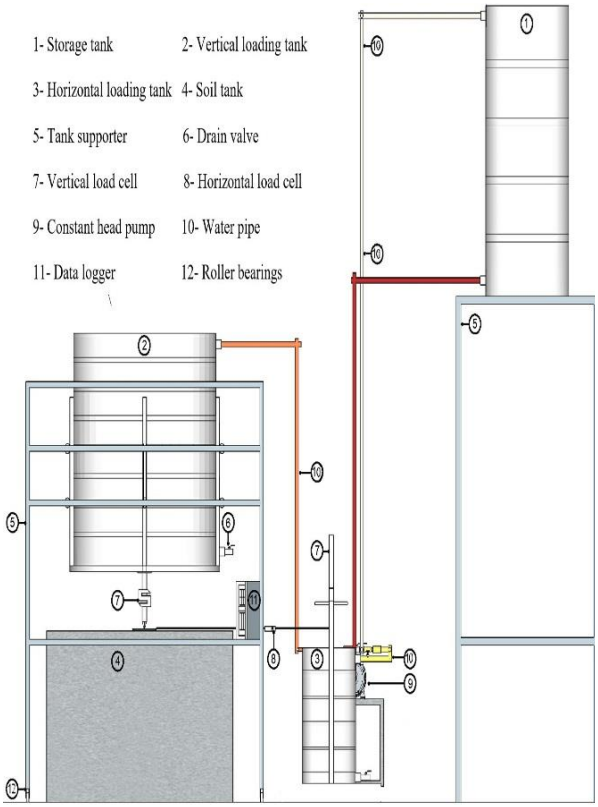

Figure 4. Schematic view of loading system

Figure 5. General photo of loading system

4. FAILURE ENVELOPE

4. 1. tan (α)-V/V$_{ult}$ Space (e=0) The failure points corresponding to V, α_C and α_V loading states are gathered in V/V$_{ult}$-tan(α) space as illustrated in Figure 6. Each point represents the failure condition of the relevant test. The trend of results shows a linear relationship between vertical load ratio (V/V$_{ult}$) and tangent of inclination angle. It has to be noted that, the α_C and α_V loading states are the loading paths parallel to horizontal and vertical axes, respectively. While the points below the failure envelope indicate the ordinary (possible) loading state and the points above that are the impossible state.

4. 2. e/B-V/V$_{ult}$ Space Tests with no inclination are considered for this space. The failure points of V, e_C, and e_V loading states are collected in the V/V$_{ult}$- e/B space as illustrated in Figure 7. The trend of results shows the linear relationship between vertical loads and eccentricity, which show the failure envelope in the V/V$_{ult}$- e/B space. It should be noted that the e_C and e_V loading states are the loading paths parallel to horizontal and vertical axes, respectively.

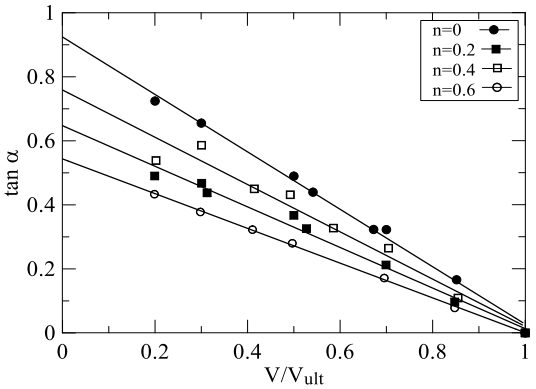

Figure 6. Failure envelopes of the ring footing in tan(α)-V/V$_{ult}$ space

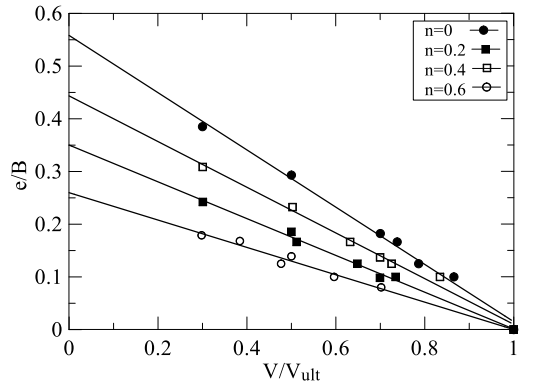

Figure 7. Failure envelopes of the ring footing in e/B-V/V$_{ult}$ space

4. 3. tan(α)- e/B Space The behavior of ring footings in the tan(α)- e/B space, which has been investigated by providing data from the α_V-e_V state test results, indicates a nonlinear relationship between tan(α)-e/B at any constant value of vertical load as illustrated in Figure 8.

The effect of the diameter ratio on the failure envelope in the tan(α)- e/B space for V= $0.5V_{ult}$ is illustrated in Figure 9. It can be observed that the results for n=0.2 appear to fall out of sequence with the other results. This could be explained by creating an additional shear failure surface, which develops from the internal edge of the ring footing and extends beyond the end of the wedge zone of the shear failure surface. However, additional shear failure surface causes the friction area of the active zone. This phenomenon is called the *edge effect*, which is also true for the optimum diameter ratio of a ring footing (n=0.4). When n>0.4, the bearing capacity is reduced because of the high interaction between both of the external and internal shear failure surfaces in the small zone (Figures 10 and 11) [27].

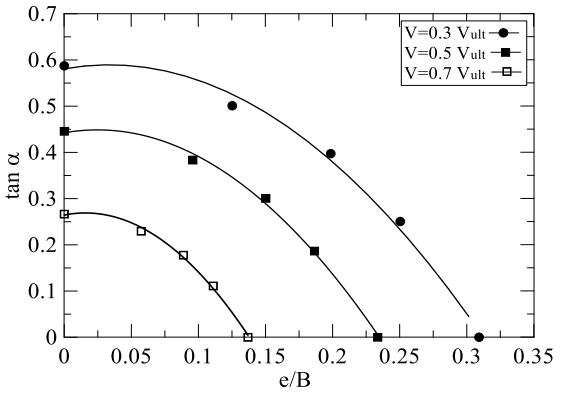

Figure 8. Failure envelopes of the ring footing in tan (α)-e/B space for different magnitude of vertical load (n=0.4)

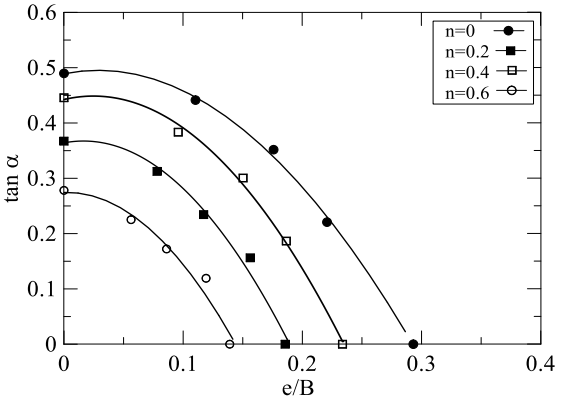

Figure 9. Failure envelopes of the ring footing in tan(α)-e/B space

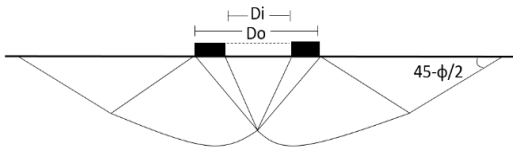

Figure 10. Ring footing edge effect (0<n≤0.4)

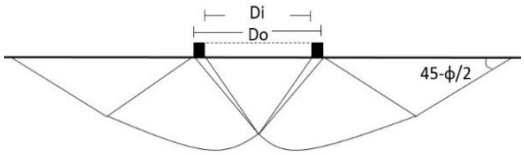

Figure 11. Ring footing edge effect (n>0.4)

5. MODEL DEVELOPMENT

To predict the behavior of ring footing subject to eccentric inclined loading, an analytical model, based on experimental results and failure envelops were developed and proposed as follows (see Equations (1)-(3)):

$$\text{In } \textit{tan } \alpha\textit{-V/V}_{ult}\textit{ space}: \tan\alpha = h\left(1-\frac{V}{V_{ult}}\right) \quad (1)$$

$$\text{In } \textit{e/B-V/V}_{ult}\textit{ space}: \frac{e}{B} = m\left(1-\frac{V}{V_{ult}}\right) \quad (2)$$

$$\text{In } \textit{tan } \alpha\textit{- e/B space}: \left(\frac{\tan\alpha}{h}\right)^2 + \left(\frac{e}{mB}\right)^2 + c\frac{\tan\alpha}{h}\frac{e}{mB} = D \quad (3)$$

where, V, V_{ult}, *e*, *B*, α are vertical load, ultimate vertical load, load eccentricity, the outer diameter of the footing model and the inclination angle, respectively. Also *h*, *m* and *c* are footing shape coefficients and *D* is a functional coefficient of V/V_{ult} ratio, i.e. (Equation (4)):

$$D = \left(1-{}^{V}/_{V_{ult}}\right)^2 \quad (4)$$

Combining Equations (1), (2) and (3), derived for the failure envelopes in 2D spaces, leads to Equation (5), which expresses the 3D shape of the failure in the V/V_{ult}-tan (α)-e/B space:

$$\left(\frac{\tan\alpha}{h}\right)^2 + \left(\frac{e}{mB}\right)^2 + c\frac{\tan\alpha}{h}\frac{e}{mB} = \left(1-{}^{V}/_{V_{ult}}\right)^2 \quad (5)$$

Using the least square method, the constant coefficients, which are derived based on the test results, are summarized in Table 2.

TABLE 2. Parameters of the failure envelope for different diameter ratios

n	h	m	c
0	1	0.6	0.2
0.2	0.7	0.35	0.2
0.4	0.8	0.45	0.2
0.6	0.28	0.14	0.2

The 3D failure envelope of ring footing diagrams based on coefficient derived from Table 2 are shown in Figure 12.

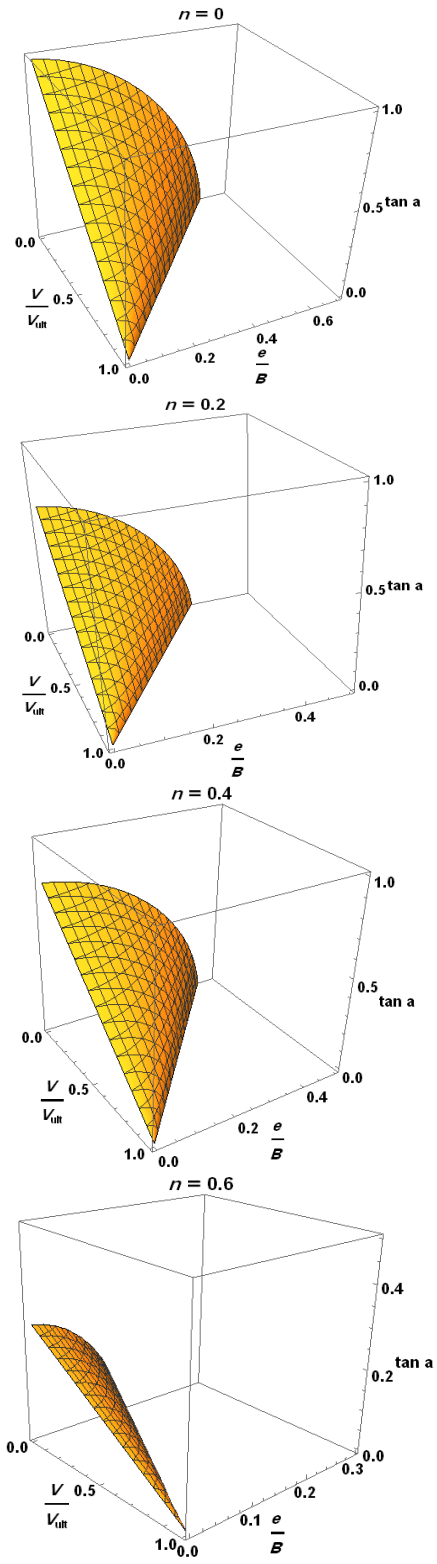

Figure 12. The 3D failure envelopes of ring footing

6. TEST RESULTS ANALYSIS

Shallow footings subjected to eccentric inclined loading can be analyzed as a combination of vertical load (V), horizontal load (H), and moment (M) simultaneously. Then, the failure envelope in V-H and M/D_o-V spaces are obtained. A noteworthy finding of this study is a new parameter called the *inclined load line*, which has a constant inclination angle in the V/V_{ult}-H/V_{ult} space and can be introduced to interpret the results as follows: Where α is the inclination angle of load with respect to the vertical direction, and the other parameters are as described earlier. When a ring footing is subjected to the inclined load with an inclination angle of α, the loading path in the V/V_{ult}-H/V_{ult} space is a line determined by Equation (6).

$$\frac{H}{V_{ult}} = \frac{V}{V_{ult}} tan\,\alpha \quad (6)$$

The intersection of this line with the failure envelope in the V/V_{ult}-H/V_{ult} space represents the positions of failure points. This helps to predict the ring footing behavior subject to the inclined loading. In addition, an increase in the value of α causes the inclined load to get closer to the vertical axis in the V/V_{ult}-H/V_{ult} space until the line becomes tangent to the failure envelope. The inclination angle of loading, which results in tangency with the failure envelope, is called the *critical angle* (α_{cr}). In the case of $\alpha \geq \alpha_{cr}$, the ring footing slid, and an instability condition occurred. Based on the test results, four inclined load lines were sketched (see Figure 13). For instance, the inclined load line with α=25° is tangent to the failure envelope of the ring footing with n=0.6. This indicates that it is not possible to apply an inclined load under these conditions. In other words, the ring footing with n=0.6 is not stable if α=25°.

Similarly, a new parameter in M/BV_{ult}-V/V_{ult} space can be defined as *eccentric load line*. This parameter is defined by Equation (7):

$$\frac{M}{BV_{ult}} = e\frac{V}{V_{ult}} \quad (7)$$

Equation (7) describes a line with a constant slope in the M/D_oV_{ult}-V/V_{ult} space. The intersection of this line with the failure envelope provides the ultimate bearing capacity of an eccentrically-loaded ring footing. As the load eccentricity increases, the line slope increases until it reaches the failure envelope. The load eccentricity in this situation is called the *critical eccentricity* (e_{cr}). When $e \geq e_{cr}$, the ring footing is unstable and vibrates in the rocking mode. For instance, as shown in Figure 14, it is not possible to apply a load with $e=D_o/4$ on a ring footing with n=0.6. Also, as the diameter ratio becomes smaller, loads with larger eccentricity can be applied to the ring footing. Based on the test results, the magnitudes of critical angle and corresponding critical eccentricity are summarized in Table 3.

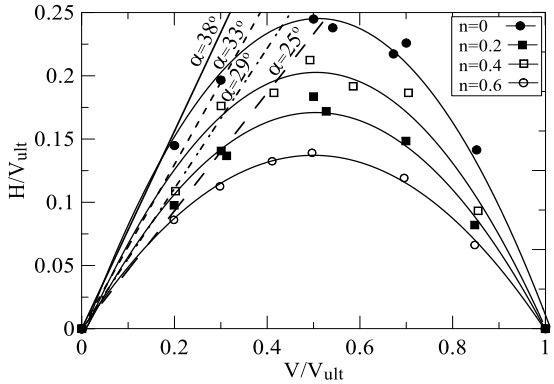

Figure 13. Inclined load lines in H/V_{ult}-V/V_{ult} space

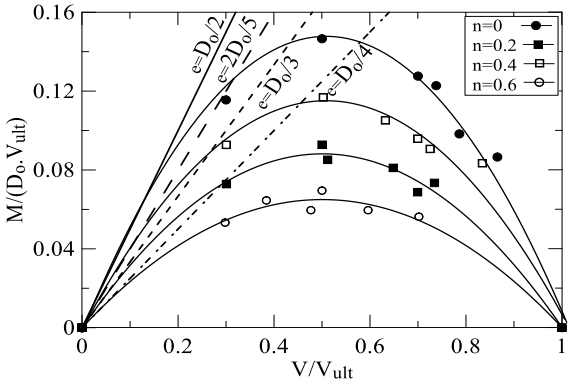

Figure 14. Eccentric load lines in M/D_oV_{ult}-V/V_{ult} space

TABLE 3. Values of the critical angle and the critical eccentricity

n	α_{cr}	e_{cr}
0	38	$D_o/2$
0.2	29	$D_o/3$
0.4	33	$2D_o/5$
0.6	25	$D_o/4$

7. VERIFICATION

To the best of authors' knowledge, no similar attempt was made to study the behavior of ring footings subject to combined loading. However, it is only possible to compare the results for vertical loading states for ring footing and combined loading state for other types of footing (such as circular and strip footings). This was conducted as follows:

7. 1. Footing Subject to Pure Vertical Loading

One method to verify the test results is to compare N_γ values of different studies using Equation (8) [12].

$$N_\gamma = \frac{q_u}{0.5B\gamma} \quad (8)$$

The obtained trend of N_γ seems to be comparable and reasonable with others findings (see Figure 15). However, the differences depend on the internal friction angle of soil as well as the approach employed in each study.

7. 2. Footing Subject to Eccentric Loading

Another way to validate the test results is to investigate the variation of a reduction factor, R_f, as expressed in Equation (9) [15].

$$R_f = \frac{q_{u,eccentric}}{q_{u,centric}} \quad (9)$$

where $q_{u,eccentric}$, $q_{u,centric}$ are the ultimate bearing capacity of the footing subject to eccentric and centric loading, respectively. As shown in Figure 16, the results of this study are generally in good agreement with those reported in other investigations.

7. 3. Footing Subject to Combined Loading

The proposed model of shallow footing subject to combined loading is presented in Equations (10) and (11) [28]. Figures 17 and 18 show the failure envelope obtained from the test results in a normalized H/H_{ult}-V/V_{ult} and

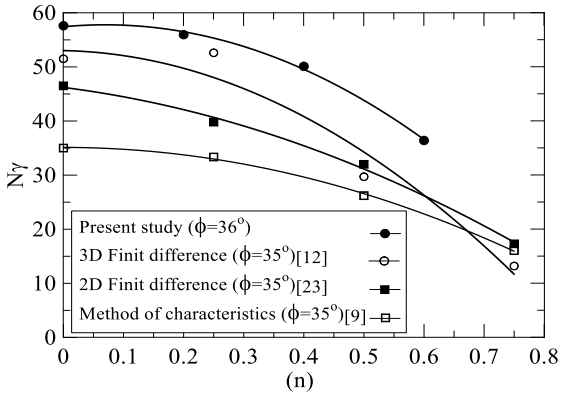

Figure 15. Variation of N_γ with the diameter ratio for a ring footing

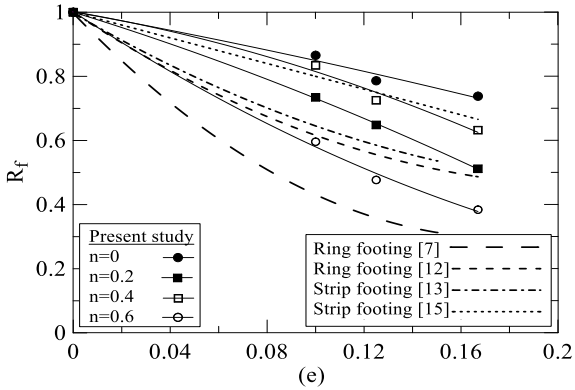

Figure 16. Variation of R_f with the eccentricity

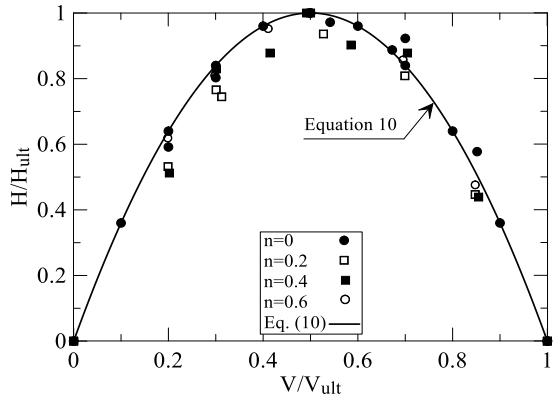

Figure 17. The failure envelope of a ring footing in H/H_{ult}-V/V_{ult} space

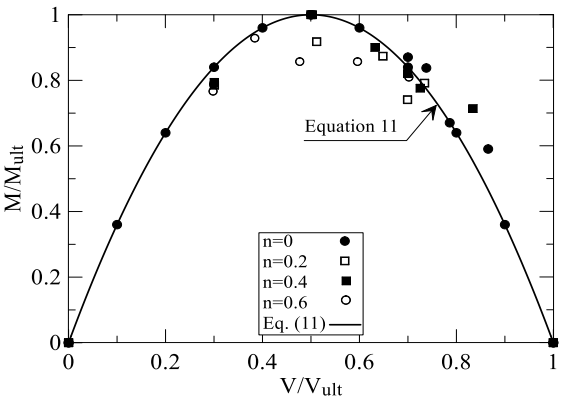

Figure 18. The failure envelope of the ring footing in M/M_{ult}-V/V_{ult} space

M/M_{ult}-V/V_{ult} space respectively, which is in a good agreement with the outputs of Equations (10) and (11).

$$\frac{H}{H_{ult}} = 4\frac{V}{V_{ult}}(1-\frac{V}{V_{ult}}) \quad (10)$$

$$\frac{M}{M_{ult}} = 4\frac{V}{V_{ult}}(1-\frac{V}{V_{ult}}) \quad (11)$$

where, all of parameters were introduced before.

8. CONCLUSION

In this study, 100 experimental tests were performed to investigate the behavior of ring footings resting on sandy soils subject to combined eccentric inclined loading. Since ring footings comprise less material than circular footings with the same outer diameter, ring footings are economically efficient in the engineering projects. In order to study the combined loading effect on the behavior of ring footings, six loading states were considered. The obtained results were described as follows:

The failure envelopes in the V/V_{ult}-tan(α) and V/V_{ult}-e/B spaces are governed by a line. Therefore, as the vertical load decreases, loading with more eccentricity becomes possible. In the same manner, when vertical load decreases, loading with a higher inclination angle is possible. Moreover, the failure envelopes in the tan(α) - e/B space are governed by a quarter ellipsoid, which is useful for the design of footings subject to eccentric inclined loading. When the eccentricity is increased, the possible inclination angle is decreased. In the same way, when the inclination angle is increased, the possible eccentricity is decreased. The constant coefficients of the failure envelope, n, m, and h, are introduced in terms of the ring footing diameter ratio. It is observed that the optimum ring footing diameter ratio is 0.4, subject to combined eccentric inclined loading. According to this result, it is more appropriate to use a ring footing with a diameter ratio of n=0.4. The geometrical shape of the 3D failure envelope in the V/V_{ult}-tan(α)-e/B space is quite similar to a cone, and its size varies with the ring footing's diameter ratio. Another advantage of the failure envelope is the control of stability conditions subject to the desired loading state. In this research, by defining the critical eccentricity and critical inclined angle, it is possible to check the stability of ring footings in the V/V_{ult}-H/V_{ult} and M/BV_{ult}-V/V_{ult} spaces. The results show that a ring footing with diameter n=0.4 is more stable than other ring footings when subjected to inclined eccentric loading.

It is worth mentioning that the main limitation of this research is the small scale of ring footing and the soil bed which a special granular material. This research could be developed on cohesive and/or saturated soil. Also a numerical approach makes it possible to evaluate all diameter ratio of ring footings subject to combined loading.

9. REFRENCES

1. Meyerhof, G. G. "The Ultimate Bearing Capacity of Foundations on Slopes La Force Portante des Fondations sur Talus." In Proceedings of the Fourth International Conference on Soil Mechanics and Foundation Engineering, (1957), 384–386. Retrieved from https://www.academia.edu/download/48325191/docslide.us_ultimate-bearing-capacity-of-foundations-on-slopes-paper.pdf
2. Meyerhof, G. G. "Influence of Roughness of Base and Ground-Water Conditions On The Ultimate Bearing Capacity of Foundations." ***Géotechnique***, Vol. 5, No. 3, (1955), 227–242. https://doi.org/10.1680/geot.1955.5.3.227
3. Hansen, J. B. "A revised and extended formula for bearing capacity." Bulletin No. 28, Copenhagen: Danish Geotechnical Institute, (1970), 5–11. Retrieved from https://trid.trb.org/view/125129
4. Egorov, K. E. "Calculation of bed for foundation with ring footing." In Proceeding 6 th International Conference of Soil Mechanics and Foundation Engineering (Vol. 2) (1965),41–45.

5. Hataf, N., and Razavi, M. R. "Model tests and finite element analysis of bearing capacity of ring footings on loose sand." ***Iranian Journal of Science and Technology, Transaction B - Engineering***, Vol. 27, No. 1, (2003), 47–56. Retrieved from https://www.sid.ir/en/Journal/ViewPaper.aspx?ID=14838
6. Boushehrian, J. H., and Hataf, N. "Experimental and numerical investigation of the bearing capacity of model circular and ring footings on reinforced sand." ***Geotextiles and Geomembranes***, Vol. 21, No. 4, (2003), 241–256. https://doi.org/10.1016/S0266-1144(03)00029-3
7. El Sawwaf, M., and Nazir, A. "Behavior of Eccentrically Loaded Small-Scale Ring Footings Resting on Reinforced Layered Soil." ***Journal of Geotechnical and Geoenvironmental Engineering***, Vol. 138, No. 3, (2012), 376–384. https://doi.org/10.1061/(asce)gt.1943-5606.0000593
8. Karaulov, A. M. "Static solution of the limiting-pressure problem for ring foundations on soil beds." ***Soil Mechanics and Foundation Engineering***, Vol. 42, No. 6, (2005), 189–194. https://doi.org/10.1007/s11204-006-0007-5
9. Kumar, J., and Ghosh, P. "Bearing capacity factor Nγ for ring footings using the method of characteristics." ***Canadian Geotechnical Journal***, Vol. 42, No. 5, (2005), 1474–1484. https://doi.org/10.1139/t05-051
10. Al-Sanad, H. A., Ismael, N. F., and Brenner, R. P. "Settlement of Circular and Ring Plates in Very Dense Calcareous Sands." ***Journal of Geotechnical Engineering***, Vol. 119, No. 4, (1993), 622–638. https://doi.org/10.1061/(ASCE)0733-9410(1993)119:4(622)
11. Laman, M., Yildiz, A., Ornek, M., and Demir, A. "Field Test of Circular Footings on Reinforced Granular Fill Layer Overlying a Clay Bed." ***Geotechnical Testing Journal***, Vol. 35, No. 4, (2012), 575–585. https://doi.org/10.1520/GTJ103512
12. Sargazi, O., and Seyedi Hosseininia, E. "Bearing capacity of ring footings on cohesionless soil under eccentric load." ***Computers and Geotechnics***, Vol. 92, (2017), 169–178. https://doi.org/10.1016/j.compgeo.2017.08.003
13. Purkayastha, R. D., and Char, A. N. "Stability analysis for eccentrically loaded footings." ***Journal of Geotechnical and Geoenvironmental Engineering***, Vol. 103, No. GT-6, (1977), 647–651. Retrieved from https://trid.trb.org/view/59977
14. Saran, S., and Agarwal, R. K. "Bearing Capacity of Eccentrically Obliquely Loaded Footing." ***Journal of Geotechnical Engineering***, Vol. 117, No. 11, (1991), 1669–1690. https://doi.org/10.1061/(ASCE)0733-9410(1991)117:11(1669)
15. Patra, C. R., Behara, R. N., Sivakugan, N., and Das, B. M. "Ultimate bearing capacity of shallow strip foundation under eccentrically inclined load, Part I." ***International Journal of Geotechnical Engineering***, Vol. 6, No. 3, (2012), 343–352. https://doi.org/10.3328/IJGE.2012.06.03.343-352
16. Loukidis, D., Chakraborty, T., and Salgado, R. "Bearing capacity of strip footings on purely frictional soil under eccentric and inclined loads." ***Canadian Geotechnical Journal***, Vol. 45, No. 6, (2008), 768–787. https://doi.org/10.1139/T08-015
17. Krabbenhoft, S., Damkilde, L., and Krabbenhoft, K. "Lower-bound calculations of the bearing capacity of eccentrically loaded footings in cohesionless soil." ***Canadian Geotechnical Journal***, Vol. 49, No. 3, (2012), 298–310. https://doi.org/10.1139/T11-103
18. Gupta, R., and Trivedi, A. "behavior of model circular footings on silty soils with cellular supports." ***International Journal of Engineering, Transactions B: Applications***, Vol. 23, No. 1, (2010), 21–35. Retrieved from http://www.ije.ir/article_71826.html
19. Safarzadeh, Z., and Aminfar, M. H. "Experimental and numerical modeling of the effect of groundwater table lowering on bearing capacity of shallow square footings." ***International Journal of Engineering, Transactions A: Basics***, Vol. 32, No. 10, (2019), 1429–1436. https://doi.org/10.5829/ije.2019.32.10a.12
20. Azan, D., and Haddad, A. "Effect of Fuzzy Boundaries on the Bearing Capacity of Footings on Two-Layered Clay." ***International Journal of Engineering, Transactions B: Applications***, Vol. 32, No. 5, (2019), 667–672. https://doi.org/10.5829/ije.2019.32.05b.07
21. Ibrahim, S. K., and Zakaria, W. A. "Effect of Vibrating Footing on a Nearby Static – Load Footing." ***Civil Engineering Journal***, Vol. 5, No. 8, (2019), 1738–1752. https://doi.org/10.28991/cej-2019-03091367
22. Moffitt, C. J. "Footing Soil Pressure from Biaxial Loading." ***Civil Engineering Journal***, Vol. 5, No. 11, (2019), 2423–2440. https://doi.org/10.28991/cej-2019-03091421
23. Jalili, M., Ghasemi, M. R., and Pifloush, A. R. "Stiffness and strength of granular soils improved by biological treatment bacteria microbial cements." ***Emerging Science Journal***, Vol. 2, No. 4, (2018), 219–227. https://doi.org/10.28991/esj-2018-01146
24. Shadmand, A., Ghazavi, M., and Ganjian, N. "Scale Effects of Footings on Geocell Reinforced Sand Using Large-Scale Tests." ***Civil Engineering Journal***, Vol. 4, No. 3, (2018), 497. https://doi.org/10.28991/cej-0309110
25. Tajeri, S., Sadrossadat, E., and Bazaz, J. B. "Indirect estimation of the ultimate bearing capacity of shallow foundations resting on rock masses." ***International Journal of Rock Mechanics and Mining Sciences***, Vol. 80, (2015), 107–117. https://doi.org/10.1016/j.ijrmms.2015.09.015
26. Abdollahi, M., and Bolouri Bazaz, J. "Reconstitution of Sand Specimens Using a Rainer System." ***International Journal of Engineering, Transactions B: Applications***, Vol. 30, No. 10, (2017), 1451–1463. https://doi.org/10.5829/ije.2017.30.10a.05
27. Jumikis, A. Theoretical soil mechanics: With practical applications to soil mechanics and foundation engineering, Van Nostrand Reinhold Company, 1969.
28. Gottardi, G., Houlsby, G. T., and Butterfield, R. "Plastic response of circular footings on sand under general planar loading." ***Géotechnique***, Vol. 49, No. 4, (1999), 453–469. https://doi.org/10.1680/geot.1999.49.4.453

Persian Abstract

چکیده

بررسی همه جانبه رفتار پی‌های حلقوی تحت بارگذاری مایل و خارج محور مبحثی است که کمتر مورد توجه محققان قرار گرفته است. در این پژوهش با استفاده از مدلسازی آزمایشگاهی، رفتار پی حلقوی با نسبت‌های قطر ۰، ۰/۲، ۰/٤ و ۰/٦ تحت بارگذاری ترکیبی مایل و خارج محور مورد بررسی قرار گرفته است. حالت‌های مختلف بارگذاری تعریف و نقاط گسیختگی در هر آزمایش تعیین گردید. با جمع‌آوری مقادیر بدست آمده سطح گسیختگی پی در فضای tan(α)-e/B-V/Vult ترسیم و معادله سطح گسیختگی بدست آمد. سپس ضرایب رابطه سطح گسیختگی با توجه به نسبت‌های مختلف قطر پی حلقوی کالیبره گردید. نتایج نشان می‌دهد با افزایش مقدار بار قائم، زاویه انحراف و گریز از مرکز کمتر امکان پذیر است. همچنین افزایش خروج از محوری بار قائم امکان بارگذاری مایل با زاویه انحراف بار کمتر را ممکن می کند. در ادامه با استفاده از مفهوم سطح گسیختگی به بررسی پایداری پی تحت بارگذاری ترکیبی مایل و خارج محور پرداخته شده است.